Electrical Engineering
https://doi.org/10.1007/s00202-021-01289-3

ORIGINAL PAPER

A new voltage regulation strategy using developed power sharing techniques for solar photovoltaic generation-based microgrids

Bilal M. Eid[1] · Josep M. Guerrero[2] · Abdullah M. Abusorrah[3] · Md. Rabiul Islam[4]

Received: 5 October 2020 / Accepted: 5 April 2021

Abstract
Integration of solar photovoltaic (PV) sources to power grid is increasing rapidly in recent years. Since the PV source is an intermittent source, this causes many challenges to distribution network. To overcome these challenges, a voltage regulation strategy using a developed power management technique for microgrid system is proposed. The technique is based on voltage ride through capability. The active and reactive power flow along with the voltage profile has been deeply investigated to improve the stability of the distribution network. As a testing environment, three microgrid configurations developed in MATLAB/Simulink have been investigated. The study shows a faster response time and lower circulating current in configuration 2. Moreover, it revealed the effectiveness of the power management technique when a cluster of dispatchable and non-dispatchable distributed generators is in operation.

Keywords Voltage regulation · Power sharing control strategies · Distributed generators · Microgrid

1 Introduction

The integration of distributed generators (DGs) became a very effective solution nowadays due to the importance of having the generators closer to the loads [1–4]. DGs can contribute to the reduction of the electrical and physical distances between loads and generators, reducing power losses and carbon emission levels in transmission and distribution. Furthermore, the bottlenecks in the distribution and transmission lines will also be removed and improve the reactive power supply to enhance grid voltage profiles and power stability. The DGs also can improve the utilization of waste heat and delay the necessity of establishing new power generation plants and transmission lines [1,5,6].

Renewable energy sources (RESs) offer superior advantages over other DGs including higher availability, zero carbon dioxide emissions, lower running and maintenance cost [4,7]. These advantages contributed to the spread of the RES into electrical power systems worldwide. As it is shown in Fig. 1 from International Renewable Energy Agency (IRENA), there is a huge growth in the renewable generation capacity worldwide, which is driven mostly by the new solar and wind installations [8]. Increasing the integration of RES causes some negative effects such as overrated voltage problem, circulating current, disturbances of the amplitude and frequency of the network's voltage and the possibility of having power flowing in the opposite direction in transmission lines [9]. The drawbacks are more obvious in case of the connection to the low-voltage electrical power network [10].

Various RES aggregations have been studied [6,7,11,12]. This study investigated the combination of PV and FC sources, which is recently attracting many researchers worldwide [13,14] due to the dispatchable power capability of

✉ Bilal M. Eid
bilal.eid@hku.edu.tr

Josep M. Guerrero
joz@et.aau.dk

Abdullah M. Abusorrah
aabusorrah@kau.edu.sa

Md. Rabiul Islam
mrislam@uow.edu.au

1 Electrical and Electronics Engineering Department, Hasan Kalyoncu University, Gaziantep, Turkey

2 Department of Energy Technology, Center of Research on Microgrids, Aalborg University, Aalborg, Denmark

3 Department of Electrical and Computer Engineering, Center of Research Excellence in Renewable Energy and Power Systems, King Abdulaziz University, Jeddah, Saudi Arabia

4 School of Electrical, Computer and Telecommunications Engineering, University of Wollongong, Wollongong, NSW 2522, Australia

Published online: 23 April 2021

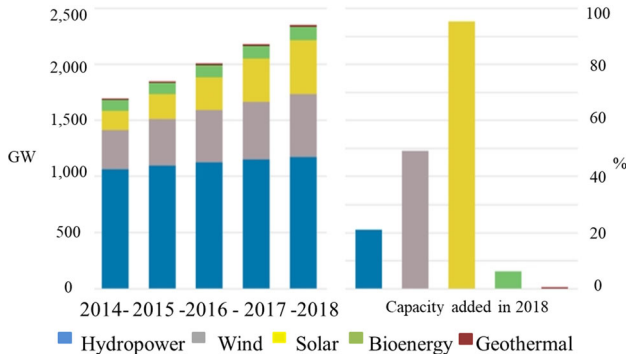

Fig. 1 Renewable generation capacity growth

the FC sources. The intermittency issue is associated with the integration of RES; this problem normally can be overcome by adding a controllable energy storage device to the microgrid [14–16]. (A microgrid is an electrical power system containing generation, storage and loads that can operate independent of the bulk power system [17].) An energy storage device, however, reduces the efficiency and the plug-and-play capability [18,19]. In addition, the lifespan of the battery is much less than the PV panels and the inverters, which are the main two important components in the solar systems. Therefore, the usage of batteries is not recommended for voltage and power regulation, and it can be replaced by DGs with fast response rate, so the intermittent PV source can be regulated [13]. The FC source is a good example for a RES with the dispatchable power capability [20].

Investigating the impacts of microgrid configuration on the power management system has been done in many past works [12,21,22]. In [12,23] multiple DGs system operating in both grid-connected and islanded modes with active power and frequency control technique have been described. In order to control the active power, two controlling modes have been introduced: unit output power control (UPC) and feeder flow control (FFC). In these studies, more than one configuration of DGs has been investigated under the following circumstances: (1) the disturbances of the load at islanded and grid-connected operation and (2) during the disconnection from the grid (the transition period). It has been found that FFC strategy has superior capability during the variation of the load [12]. However, a source with dispatchable power capability was only used in that paper; moreover, the simulation's results were achieved only for one configuration without showing the circulating reactive power along with the voltage profile in whole buses.

Two configurations were investigated in [21]; each configuration consists of two subsystems with a control system in each. In every subsystem, a wind turbine and a solar PV source, along with a local load, are available. The difference between the configurations is that configuration number 1 can exchange the generated power inside the microgrid, while the other must exchange the whole generated power with the distribution network. The purpose of the analysis in [21] was to compare power transfers of the two configurations with the main grid and to investigate how the connection of subsystems affects the distribution network from dependency and energy security point of view. However, the reactive power and voltage regulation have not been investigated in this study.

In [24], ac and dc microgrid time dependence effects in the distribution network during a full day of operation have been investigated. It proposed a general configuration for a microgrid that has advantages such as improved reliability of nodal, smooth integration for dc source and lower cost. However, [24] only studied one configuration without illustrating the relation between the voltage stability and reactive power flow. In order to achieve a tie re-closer functions, a microgrid with auto-loop was utilized in [25] to reconfigure the distribution network. The microgrid with auto-loop is able to inject or absorb the power from the grid, because of which it provides high flexibility compared to ordinary auto-loops. However, [25] did not illustrate how is the connection within the microgrid, or investigated the impacts of having variant mixture of DGs, neither showed the relation between the power management and voltage regulation at the point of common coupling (PCC). A list of voltage controlling techniques for grid-connected PV generators were studied in [11]. A reactive power injection strategy was proposed by the paper as a rapid and not costly solution. However, there was no investigation for the P and Q power passing in the internal buses of the microgrids.

In order to overcome the aforementioned shortages, a microgrid controlling strategy for active and reactive regulation and voltage stability is proposed. This paper investigates a reactive power injection technique and develops a voltage regulating strategy. The influence of microgrid configurations on voltage stability, active power injection and circulating reactive power is studied as well. Three microgrid configurations connecting the DGs in different connection points have been developed to study the developed controller. A microgrid with high penetration of renewables (such as PV and FC generators) with an improved reactive power injection technique is proposed to improve distribution network and load's voltage stability.

The rest of this paper is organized as follows: Sect. 3 describes the controller of voltage and reactive power; Sect. 2 describes the microgrid design and architecture; Sect. 4 presents the simulation results and discussion; and Sect. 5 concludes the paper and suggests possible future work.

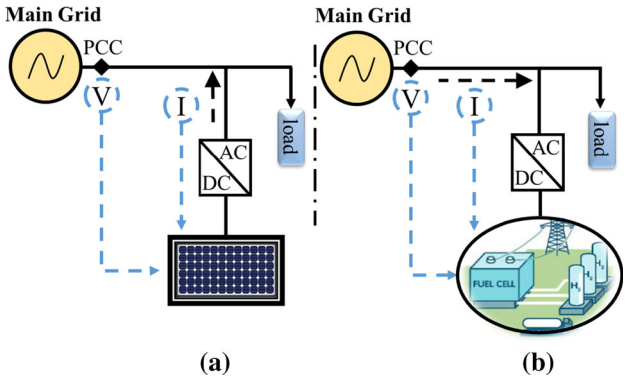

Fig. 2 **a** Unit output reactive power control mode, **b** feeder flow control mode

2 Voltage and reactive power control

Each inverter of the RES has nested control loops (inner and outer) as proposed by many researchers [19,23,26,27]. The inner loop is placed to control the current, whereas the outer loop is a voltage control loop, which works on the voltage error and setting the required current for the inner loop [19,23,28,29].

In order not to overload the RES or to deep discharge/overcharge any energy storage device, power sharing inside the microgrid has to be managed very well. This will support frequency and voltage regulation as well [29]. This can be achieved by the controlling data received from the central controller of the microgrid if the communication network is available. However, the local controller has to be designed to anticipate communication network failure. At this situation, the power sharing has to rely on the local measurement only.

2.1 Unit output reactive power control mode

In this technique, the controller operates to keep the reactive power constant at the output of the inverter, regardless the reactive power at the feeder. This technique is shown in Fig. 2a. This technique has been used in PV DGs to keep the injected reactive power zero.

2.2 Feeder flow control mode

In this technique, the controller operates to keep the reactive power constant at the main feeder, regardless the reactive power at the output of the inverter. This technique is shown in Fig. 2b. This technique has been used in FC DGs to inject the required reactive power for voltage regulation. The flowchart of the proposed control strategy is illustrated in Fig. 3. In the flowchart, the root mean square (RMS) voltage at load bus is $V_{\mathrm{BL,mes}}$ and the reference voltage is $V_{\mathrm{BL,ref}}$.

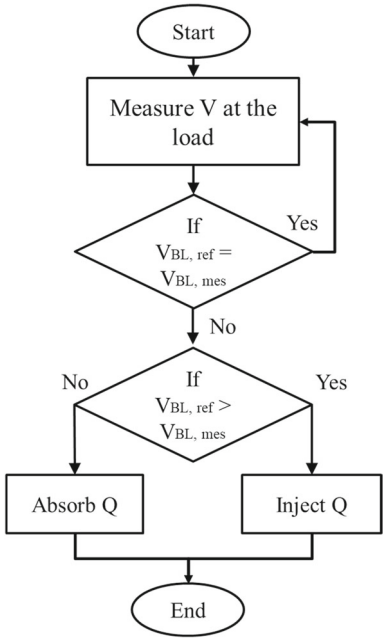

Fig. 3 Flowchart of the proposed control strategy

In this strategy, the $V_{\mathrm{BL,mes}}$ is regulated by following a specific reactive power injection formula.

2.3 Controller technique during normal operation $Q = 0$

The reactive power dispatched from the RES is controlled by the inner-loop controller. For this controller, the reference reactive current ($I_{\mathrm{q,ref}}$) is set to be zero or a fixed value to maintain the power dispatched from the RES at unity power factor. This technique is used in unit output reactive power control mode shown in Fig. 2a.

2.4 Controller technique during abnormal operation $Q \neq 0$

The controller technique during abnormal operation gives dynamic reactive power from the inverter in order to regulate the power factor at the feeder. In this operation mode, the reference reactive power ($I_{\mathrm{q,ref}}$) has a dynamic value in FC source to stabilize the voltage at load bus. The cases are shown in Eq. 1. In case (a) no action is required, in case (b) the reactive power needs to be absorbed, and in case (c) the reactive power needs to be dispatched to the grid.

$$I_{\mathrm{q,ref}} = \begin{bmatrix} 0 & \text{case } (a)\ V_{\mathrm{BL,mes}} = V_{\mathrm{BL,ref}} \\ 0 \rightarrow -1.5 & \text{case } (b)\ V_{\mathrm{BL,mes}} > V_{\mathrm{BL,ref}} \\ 0 \rightarrow 1.5 & \text{case } (c)\ V_{\mathrm{BL,mes}} < V_{\mathrm{BL,ref}} \end{bmatrix} \quad (1)$$

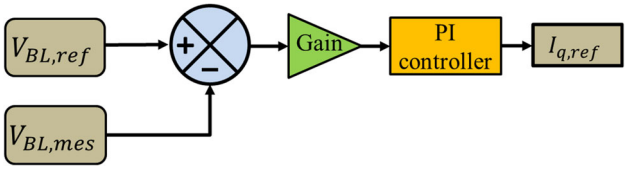

Fig. 4 Reactive power controller at FC source

where $V_{\mathrm{BL,mes}}$ is the measured value of the voltage at the load bus and $V_{\mathrm{BL,ref}}$ is the reference value of the voltage at the load bus. The value of 1.5 is 5 is the maximum value of the limiter used inside the controller.

3 Microgrid design and architecture

During the implementation of microgrid, many renewable DGs can be installed without rewiring the distribution electrical grid [2,30]. The simplicity and reasonable investment cost of the micro-DGs have made it widespread. However, large-scale DGs have more attraction for investors due to their lower cost per each installed kilo watt. This led to more large-scale renewable energy projects worldwide. An example for a large-scale operating microgrid is installed in California, USA [31]. It consists three DGs: PV source of 1.2 MW, FC source of 1 MW and diesel generators 2*1.2 MW. Another example is in Ontario Canada, which consists of wind turbine with 2.5 MVA and a synchronous generator with 2.5 MVA [32]. Both of the above-mentioned projects are grid-connected. A battery as an energy storage device has been used in the project in California, with 2 MW and 4 MWh capacity. The recommended microgrids in this work and its parameters are explained in the following sections.

3.1 Fuel cell distributed generator

The chemical energy in oxygen (O_2) and hydrogen (H_2) can be converted to electrical energy by using FC systems. In this study, a 1.1 MW FC system consisted from a cluster of 5.5 kW tubular solid oxide fuel cell (SOFC) stacks which is reported in [33] has been used. In the current FC system, 10 strings of 5 FC stacks connected in series to generate 1100 V have been used.

3.2 PV distributed generator

A solar PV DG with 1.037 MW installed capacity is used in this work. Nine of these generators are connected in parallel. This connection generated a total of 9.3 MW at 1000 W/m^2 sun irradiation. In this simulation, the V_{oc}, I_{sc}, V_{mp} and I_{mp} of the used PV panels are 64.2 V, 5.96 A, 54.7 V and 5.58 A, respectively. To form the PV source, 17 PV panels connected in series, and a total of 200 strings are connected in parallel.

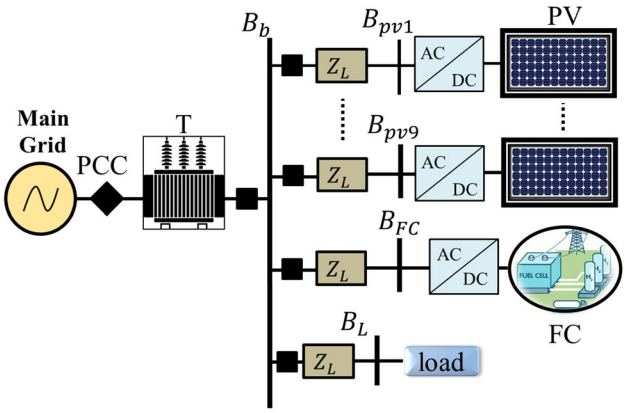

Fig. 5 Configuration 1, all DGs are connected to the common connection point

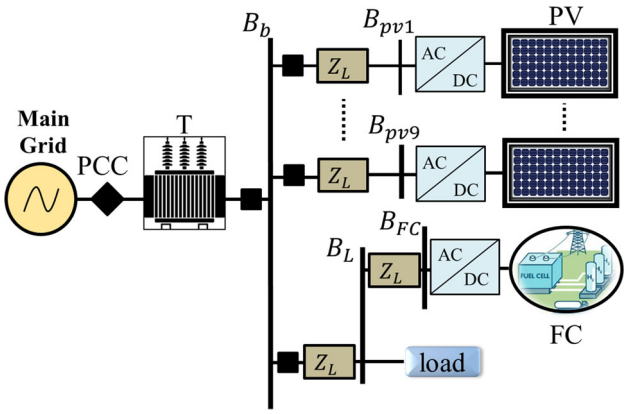

Fig. 6 Configuration 2, FC is connected to the load bus

3.3 Three microgrid configurations

The DGs inside the microgrid are connected in different connection points to investigate the effectiveness of the controller. Figure 5 shows that the DGs are connected to the common connection point at the lower voltage side of the transformer, in Fig. 6, the FC source is connected to the load bus, and in Fig. 7, the PV sources are connected in parallel and they are connected to the load bus.

The transformer connecting the grid to the microgrid has voltage ratios of 11 kV and 415 V RMS (line to line). The RES explained in Sects. 3.1 and 3.2 has been used in all proposed configurations below. The connected load has initial value of 2 MW, and the (Z_L) is representing the impedance of the distribution line.

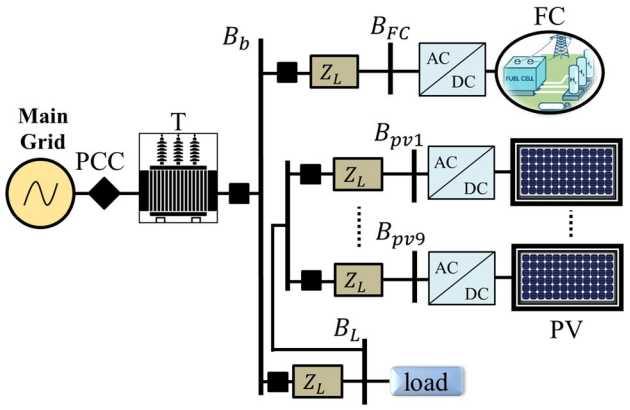

Fig. 7 Configuration 3, PV sources connected to the load bus

Table 1 Solar irradiation variation

Radiation W/m^2	Time (s)	
	From	To
1000	0	2
700	2	4
900	4	5

4 Simulation results and discussion

Due to some economic and environmental reasons, the distance between the DG and the PCC can be far. That's why in this study the effect of the distribution line distance has been considered. In some cases, the long distance can negatively affect the stability of the power system by generating resonance, power loss, poor communication between DGs and short-circuit current [17,34,35].

In the simulated cases below, the inverter controller fixed the dc V_{ref} at 930 V and 1100 V for the PV source and the FC source, respectively. In the PV source, the injected reactive power to PCC was set to be zero during the simulation, whereas the injected reactive power from the FC source has a regulated value to achieve the voltage regulation aim at the PCC. Table 1 shows the solar irradiation variation during the simulation. The initial value of the load is 2 MW, and then a 0.4 MW and 0.2 MVar load connected at 2.5 s then disconnected at 3.5 s. The value of the DC-link capacitor is 24 mF. The simulated cases are shown in the sections below:

4.1 Configuration one: all DGs to the common connection point

In this case, all the sources and load are connected to B_b, as shown in Fig. 5. In this case, the PV source used the strategy shown in Fig. 2a, whereas the FC source used the strategy shown in Fig. 2b. In Figs. 8, 9, 11, 12, 14 and 15, the dashed blue line represents the active power, while the black line depicts the reactive power.

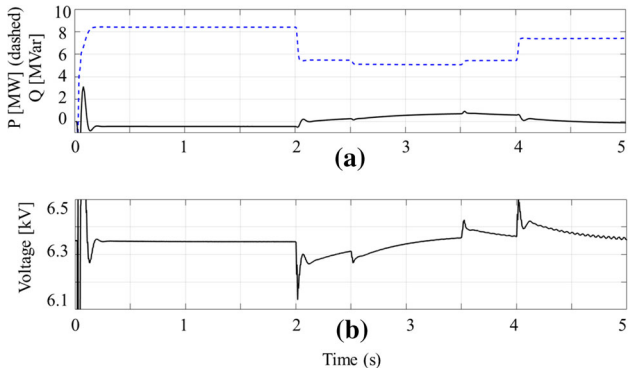

Fig. 8 Voltage, active and reactive power at the PCC, case one

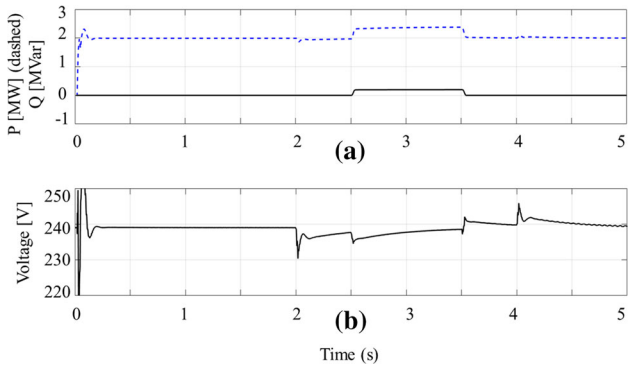

Fig. 9 Voltage, active and reactive power at the load bus, case one

In Fig. 8 the voltage at PCC, active power transferred to the grid and reactive power injected to the grid are shown. The voltage at PCC is stable between ± 2% which is within the standard limit. The drop in the active power at 2 s, 2.5 s is due to the drop in the solar radiation and the load connection, respectively.

In Fig. 9 the voltage at load, active power of the load and reactive power of the load are shown. The voltage at the load is stable between ± 2% which is within the standard limit. The increasing in the active power at 2.5 s is due to the connection of extra 0.4 MW to the load. The increasing in the active power at 2.5 s is due to the connection of extra 0.2 MVar to the load.

In Fig. 10 the voltage and reactive power in the DGs buses with and without the developed strategy are shown. It shows the dynamic value of the injected reactive power desired to stabilize the voltage in the load bus. The injected reactive power with the proposed strategy is shown in the blue dashed line. At 2 s, when the solar irradiation drops the voltage drops as well, the injected reactive power—shown in (a)—can regulate the voltage. The opposite occurs when the solar irradiation increased at 4 s. When the load connected at 2.5 s, another voltage drop occurred, while when the load removed at 3.5 s, the voltage increased and in the

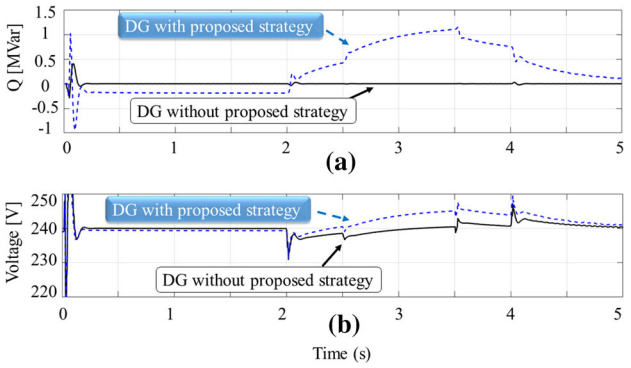

Fig. 10 Voltage and reactive power at the DGs with and without the proposed strategy, case one

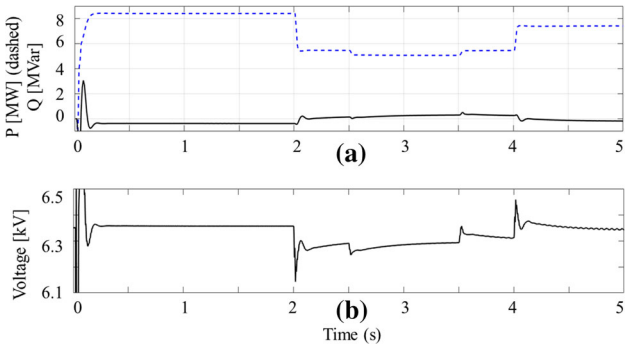

Fig. 11 Voltage, active and reactive power at the PCC, case two

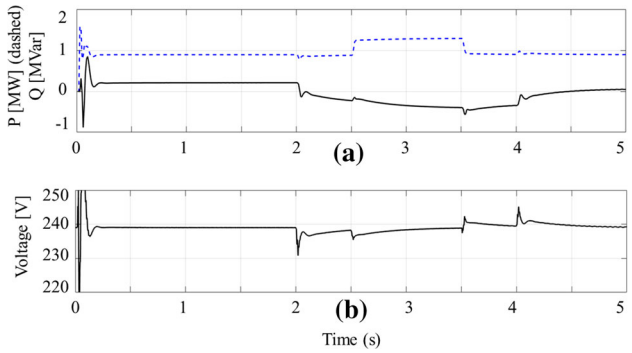

Fig. 12 Voltage, active and reactive power at the load bus, case two

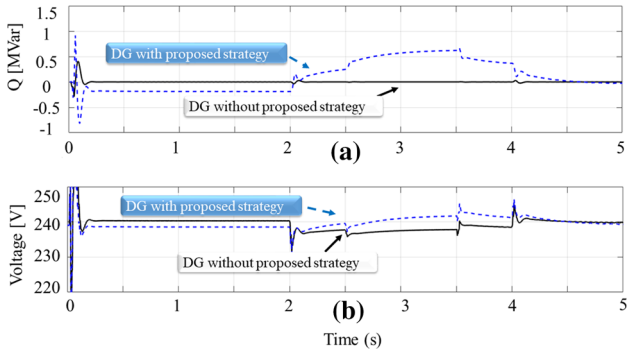

Fig. 13 Voltage and reactive power at the DGs with and without the proposed strategy, case two

both above-mentioned cases the reactive power controller reacted effectively to regulate the voltage.

4.2 Configuration two: FC to the load bus

In this case, FC is connected to the load bus as shown in Fig. 6. In this case, the PV source uses unit output reactive power control mode, while the FC source uses the feeder flow control mode.

In Fig. 11 the voltage at PCC, active power transferred to the grid and reactive power injected to the grid are shown. The voltage at PCC is stable between ± 2% which is within the standard limit. The drop in the active power at 2 s and 2.5 s is due to the drop in the solar radiation and the load connection, respectively.

In Fig. 12 the voltage at load, active power of the load and reactive power of the load are shown. The voltage at the load is stable between ± 2% which is within the standard limit. The increasing in the active power at 2.5 s is due to the connection of extra 0.4 MW to the load. The increasing in the active power at 2.5 s is due to the connection of extra 0.2 MVar to the load.

In Fig. 13 the voltage and reactive power in the DGs buses with and without the developed strategy are shown. It shows the dynamic value of the injected reactive power desired to stabilize the voltage in the load bus. The injected reactive power with the proposed strategy is shown in the blue dashed line. At 2 s, when the solar irradiation drops the voltage drops as well, so the injected reactive power—shown in (a)—can regulate the voltage. The opposite occurs when the solar irradiation increased at 4 s. When the load connected at 2.5 s, another voltage drop occurred, while when the load removed at 3.5 s, the voltage increased and in the both above-mentioned cases the reactive power controller reacted effectively to regulate the voltage. In this case, the amount of injected reactive power is less than the one shown in Fig. 10a.

4.3 Configuration three: PV to the load bus

In this case, PV sources are connected to the load bus as shown in Fig. 7. In this case, the PV source uses unit output reactive power control strategy shown in Fig. 2a, whereas the FC source uses the feeder flow control strategy shown in Fig. 2b.

In Fig. 14 the voltage at PCC, active power transferred to the grid and reactive power injected to the grid are shown. The voltage at PCC is stable between ± 2% which is within the standard limit. The drop in the active power at 2 s and

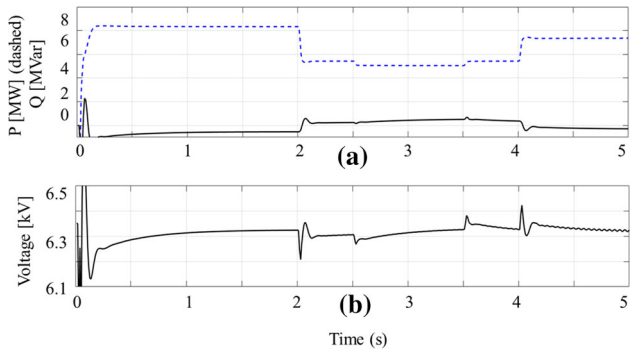

Fig. 14 Voltage, active and reactive power at the PCC, case three

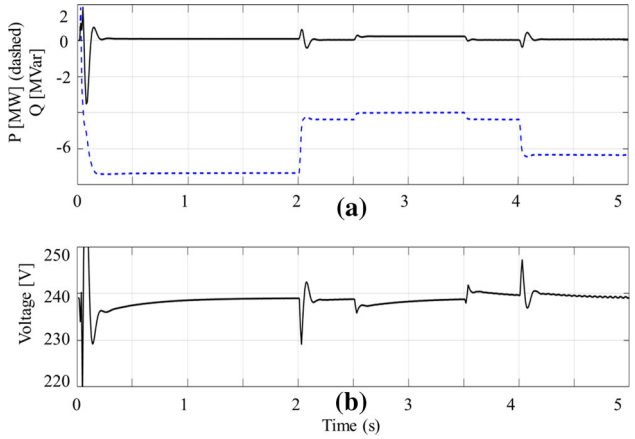

Fig. 15 Voltage, active and reactive power at the load bus, case three

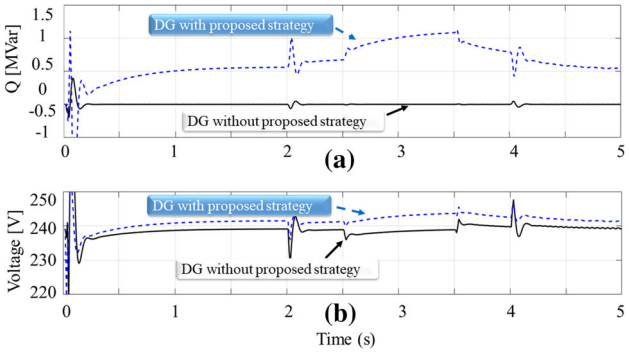

Fig. 16 Voltage and reactive power at the DGs with and without the proposed strategy, case three

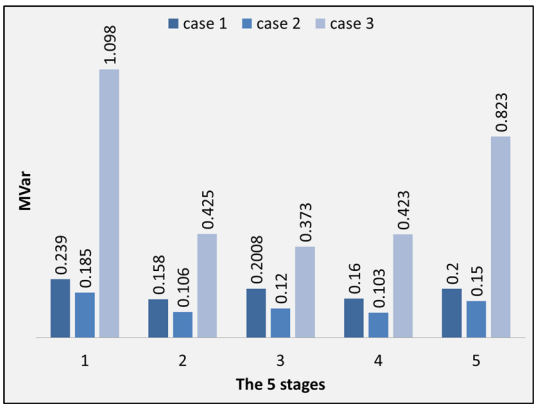

Fig. 17 Reactive power losses in the microgrid—all three cases

2.5 s is due to the drop in the solar radiation and the load connection, respectively.

In Fig. 15 the voltage at load, active power of the load and reactive power of the load are shown. The voltage at the load is stable between $\pm$ 2% which is within the standard limit.

In Fig. 16 the voltage and reactive power in the DGs buses with and without the developed strategy are shown. It shows the dynamic value of the injected reactive power desired to stabilize the voltage in the load bus. The injected reactive power with the proposed strategy is shown in the blue dashed line. At 2 s, when the solar irradiation drops the voltage drops as well, so the injected reactive power—shown in (a)—can regulate the voltage. The opposite occurs when the solar irradiation increased at 4 s. When the load connected at 2.5 s, another voltage drop occurred, while when the load removed at 3.5 s, the voltage increased and in the both above-mentioned cases the reactive power controller reacted effectively to regulate the voltage.

4.4 Results' comparison

Each case had been studied during disturbances in load and irradiation. These disturbances can be summarized in the below five stages: (1) initial stage the normal operation, (2) after the drop of the solar irradiation, (3) after the load increasing, (4) after load decreasing and (5) after solar irradiation increasing. In the figures, below cases 1, 2 and 3 compare the results of the three configurations described above.

Figure 17 compares the reactive power losses in the three cases. The highest circulating reactive power was in case three because of the higher distance between B_{FC} (the bus where the reactive power injected) and B_L (the bus where the voltage stabilization is required). From Fig. 17 also, it is shown that case 2 has the lowest reactive power losses.

In Fig. 18 the exported/imported reactive power from the grid in the five stages is shown. In stage 1 the microgrid absorbed reactive power from the public grid in all cases. However, in stages 2, 3 and 4 when the radiation dropped, the reactive power flowed from microgrid to the distribution network. From the figure, it is clear that the imported/exported reactive power has the minimum value in case 2, due to the implementation of the developed strategy at the FC generator.

In Fig. 19 the reactive power injected from B_{FC} in the three cases is shown. From the figure, it is clear that the highest reactive power occurred in case 3, whereas in case 2 the lowest reactive power occurred. Determining the amount of

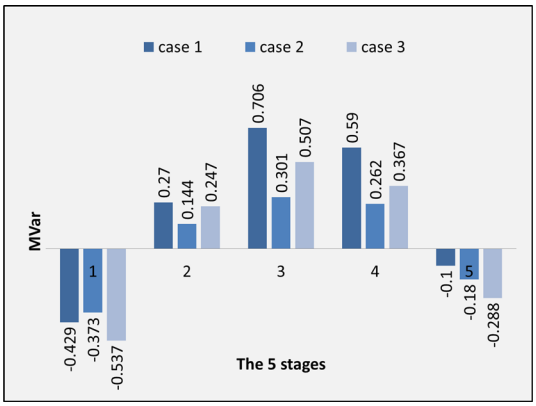

Fig. 18 Injected reactive power to the distribution network—all three cases

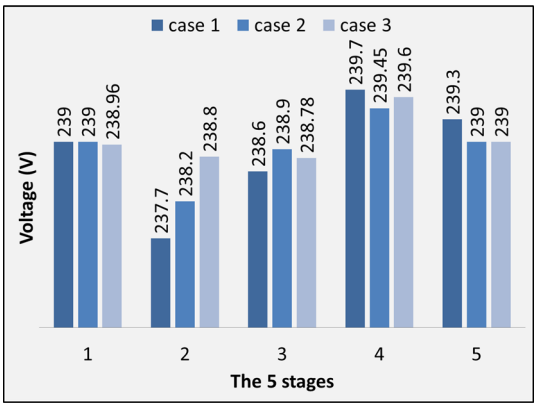

Fig. 20 RMS voltage at load—all three cases

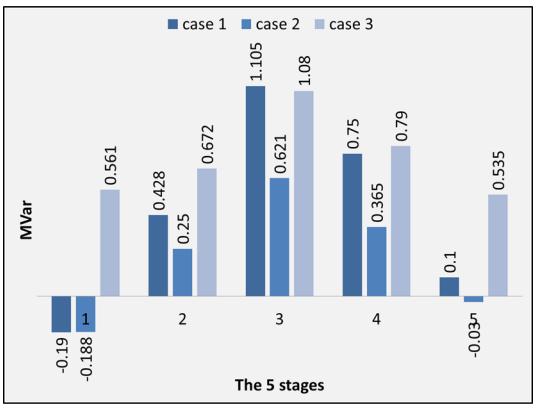

Fig. 19 Reactive power dispatched from B_{FC}—all three cases

reactive power the distance between B_{FC} and B_L is playing the main role. At initial condition (stage 1) B_{FC} absorbed reactive power at cases 1 and 2, whereas in case 3 a high amount of reactive power injected. After all disturbances at stage 5, the dispatched reactive power from B_{FC} for case 2 is insignificant. It is shown that case 2 has the lowest required reactive power to be dispatched for voltage regulation.

In Fig. 20 the voltage at load bus B_L is illustrated. The figure is showing the value of the line-to-line voltage at all cases (that represent all the configurations) and at the five stages. The voltage regulator worked properly in all cases. However, it is clear that the case 1 requires more time to reach the steady-state condition compared to the other cases.

5 Conclusions

This paper proposed a developed power management strategy to mitigate the distribution network instability due to the high PV penetration. The active and reactive power flow along with the voltage profile had been deeply investigated under disturbances scenarios—solar irradiation and load disturbances. Three microgrid configurations developed in MATLAB/Simulink have been investigated. The study showed a faster response time and lower circulating current in configuration 2. Moreover, the proposed strategy had enhanced the voltage profile at the load bus. Changing the configuration has no effect on the active power loss, while the distance between B_{FC} (Q injection bus) and B_L (voltage regulated bus) played the major role in increasing the circulating reactive power in configuration 3. The study revealed the effectiveness of the power management technique when a cluster of dispatchable and non-dispatchable DGs is in operation. When multi-microgrid connected to the distribution network, an investigation for the transformer tap changer's effects on minimizing the reactive power required for voltage regulation is recommended as a future study.

Acknowledgements This project was funded by the Deanship of Scientific Research (DSR), King Abdulaziz University, Jeddah, under Grant No. RG-22-135-41. The authors, therefore, gratefully acknowledge DSR technical and financial support. JM Guerrero was funded by a Villum Investigator Grant (No. 25920) from The Villum Fonden. The authors would also like to thank Hasan Kalyoncu University, University of Wollongong and Aalborg University for the technical assistance received.

References

1. McDonald L, Ahmadi AR, Do S, Georgiopoulos S (2017) Enabling distributed energy resources to enter the energy market and supporting the evolution to a distribution system operator. CIRED Open Access Proc J 2017(1):2715–2718
2. Mandal K, Banerjee S (2015) Synchronization phenomena in interconnected power electronic systems. IEEE Trans Circuits Syst II Express Briefs 63(2):221–225
3. Nassif AB (2018) An analytical assessment of feeder overcurrent protection with large penetration of distributed energy resources. IEEE Trans Ind Appl 54(5):5400–5407
4. Gholami S, Saha S, Aldeen M (2018) Fault tolerant control of electronically coupled distributed energy resources in microgrid systems. Int J Electr Power Energy Syst 95:327–340

5. Wang J, Zhong H, Tang W, Rajagopal R, Xia Q, Kang C (2018) Trilevel expansion planning for transmission networks and distributed energy resources considering transmission cost allocation. IEEE Trans Sustain Energy 99:1–1
6. Zhou X, Zhou L, Chen Y, Guerrero JM, Luo A, Wu W, Yang L (2018) A microgrid cluster structure and its autonomous coordination control strategy. Int J Electri Power Energy Syst 100:69–80
7. Abedini M, Moradi MH, Hosseinian SM (2016) Optimal management of microgrids including renewable energy scources using gpso-gm algorithm. Renew Energy 90:430–439
8. Statistics RC (2019) International renewable energy agency (Irena), March 2019
9. Ahmad A, Ullah N, Ahmed N, Ibeas A, Mehdi G, Herrera J, Ali A (2019) Robust control of grid-tied parallel inverters using nonlinear backstepping approach. IEEE Access 7:111982–111992
10. Farhangi H (2010) The path of the smart grid. IEEE Power Energy Mag 8(1):18–28
11. von Appen J, Braun M, Stetz T, Diwold K, Geibel D (2013) Time in the sun: the challenge of high pv penetration in the german electric grid. IEEE Power Energy Mag 11(2):55–64
12. Ahn S, Park J, Chung I, Moon S, Kang S, Nam S (2010) Power-sharing method of multiple distributed generators considering control modes and configurations of a microgrid. IEEE Trans Power Deliv 25(3):2007–2016
13. Khanh LN, Seo J-J, Kim Y-S, Won D-J (2010) Power-management strategies for a grid-connected pv-fc hybrid system. IEEE Trans Power Deliv 25(3):1874–1882
14. Elsied M, Oukaour A, Gualous H, Hassan R (2015) Energy management and optimization in microgrid system based on green energy. Energy 84:139–151
15. Koohi-Kamali S, Rahim N, Mokhlis H (2014) Smart power management algorithm in microgrid consisting of photovoltaic, diesel, and battery storage plants considering variations in sunlight, temperature, and load. Energy Convers Manag 84:562–582
16. Fossati JP, Galarza A, Martín-Villate A, Fontán L (2015) A method for optimal sizing energy storage systems for microgrids. Renewable Energy 77:539–549
17. Johnson BB, Dhople SV, Hamadeh AO, Krein PT (2014) Synchronization of nonlinear oscillators in an lti electrical power network. IEEE Trans Circuits Syst I Regul Pap 61(3):834–844
18. Hong J, Yin J, Liu Y, Peng J, Jiang H (2019) Energy management and control strategy of photovoltaic/battery hybrid distributed power generation systems with an integrated three-port power converter. IEEE Access 7:82838–82847
19. Eid BM, Rahim NA, Selvaraj J, El Khateb AH (2016) Control methods and objectives for electronically coupled distributed energy resources in microgrids: a review. IEEE Syst J 10(2):446–458
20. Jabir M, Mokhlis H, Muhammad MA, Illias HA (2019) Optimal battery and fuel cell operation for energy management strategy in mg. IET Gener Transm Distrib 13(7):997–1004
21. Mikati M, Santos M, Armenta C (2013) Electric grid dependence on the configuration of a small-scale wind and solar power hybrid system. Renew Energy 57:587–593
22. Zamora R, Srivastava AK (2018) Multi-layer architecture for voltage and frequency control in networked microgrids. IEEE Trans Smart Grid 9(3):2076–2085
23. Ziouani I, Boukhetala D, Darcherif A-M, Amghar B, Abbassi IE (2018) Hierarchical control for flexible microgrid based on three-phase voltage source inverters operated in parallel. Int J Electr Power Energy Syst 95:188–201
24. Teimourzadeh BP, Shahparasti M, Parsa MM, Haghifam MR, Mohamadian M (2014) Energy management and operation modelling of hybrid ac-dc microgrid. Gener Transm Distrib IET 8(10):1700–1711
25. Hong T, De León F (2015) A reconfigurable auto-loop microgrid. IEEE Trans Power Deliv 30(3):1644–1645
26. Green TC, Prodanović M (2007) Control of inverter-based microgrids. Electr Power Syst Res 77(9):1204–1213
27. Jaalam N, Rahim N, Bakar A, Eid B (2017) Strategy to enhance the low-voltage ride-through in photovoltaic system during multimode transition. Sol Energy 153:744–754
28. Peng F, Li Y, Tolbert L (2009) Control and protection of power electronics interfaced distributed generation systems in a customer-driven microgrid. In: Power and energy society general meeting PES'09. IEEE. IEEE 2009. pp 1–8
29. Wen S, Wang S, Liu G, Liu R (2019) Energy management and coordinated control strategy of pv/hess ac microgrid during islanded operation. IEEE Access 7:4432–4441
30. Lasseter RH (2011) Smart distribution: coupled microgrids. In: Proceedings of the IEEE, vol 99, No. 6
31. Alegria E, Brown T, Minear E, Lasseter RH (2014) Certs microgrid demonstration with large-scale energy storage and renewable generation. IEEE Trans Smart Grid 5(2):937–943
32. Arani, MF, Mohamed Y-R (2015) Analysis and impacts of implementing droop control in dfig-based wind turbines on microgrid/weak-grid stability
33. Wang C, Nehrir M (2007) A physically based dynamic model for solid oxide fuel cells. IEEE Trans Energy Convers 22(4):887–897
34. Krishna A, Schiffer J, Monshizadeh N, Raisch J (2019) A consensus-based voltage control for reactive power sharing and pcc voltage regulation in microgrids with parallel-connected inverters. In: 18th European control conference (ECC). IEEE 2019. pp 542–547
35. Ustun TS, Ozansoy C, Zayegh A (2011) Recent developments in microgrids and example cases around the world—a review. Renew Sustain Energy Rev 15(8):4030–4041